

Multiperiod fringe projection interferometry using a backpropagation method for surface profile measurement

Hai Huan,^{1,*} Osami Sasaki,² and Takamasa Suzuki²

¹Graduate School of Science and Technology, Niigata University, Niigata-shi 950-2181, Japan

²Faculty of Engineering, Niigata University, Niigata-shi 950-2181, Japan

*Corresponding author: haihuan@gmail.com

Received 7 March 2007; revised 29 August 2007; accepted 30 August 2007;
posted 5 September 2007 (Doc. ID 80736); published 8 October 2007

Interference fringes with different periods are projected on an object surface. There is a constant phase point where the phase of the fringe is kept at a constant value while the period is scanning. Multiple optical fields with different periods on the object surface are made from detected phases of the fringes. The multiple optical fields are backpropagated to the constant phase point of the phase where all of the phases of the multiple backpropagated fields become the same value and the amplitude of the sum of the multiple backpropagated fields becomes maximum. The distance of the backpropagation provides the position of the object surface. Some experiments show that this method can measure an object surface with discontinuities of several millimeters with high accuracy of several micrometers. © 2007 Optical Society of America

OCIS codes: 120.2650, 120.6650, 120.3180.

1. Introduction

Moiré and fringe projection techniques are noncontact optical techniques that have been widely applied in industry for measuring the 3D profile of object surfaces [1]. These two techniques use the fringe patterns projected onto the object surfaces, which are generated with either a grating or two laser beams. The surface profile of the object is obtained from a phase distribution of the fringe patterns which is calculated by the Fourier transform method [2] or by the phase-shifting method [3]. Since the phase distribution of the fringe pattern lies in the range from $-\pi$ to π , spatial phase unwrapping must be carried out to recover the surface profile. However, since the phases of two adjacent measurement points are compared and connected in spatial phase unwrapping, it is impossible to recover the surface profile with discontinuities such as height steps or spatially isolated surfaces, which cause phase jumps larger than 2π . The moiré and fringe projection techniques using only one-period fringe projection are difficult to measure object surfaces with the discontinuities.

Recently some methods [4–10] using multiperiod fringe projection have been proposed to measure object surfaces with the discontinuities. These methods have some analogy with multiwavelength interferometer techniques [11–13]. One basic idea of the multiperiod fringe projection technique is to use a fringe pattern with a large period, which makes the phase jump smaller than 2π for the spatial phase unwrapping. Since the measurement accuracy is not high when the period of the fringe is large, fringe patterns of small periods are used to improve the accuracy. A simple method based on this idea has been reported in [4] in which just two different periods were used. This idea was developed by using fringe patterns of several periods for measuring discontinuous objects with a higher accuracy as described in [5]. Another basic idea of multiperiod fringe projection technique is to use the intensity or phase change of the projected fringe pattern on each measurement point of the object surface when the fringe period is scanned. A method using the intensity change in a shadow moiré profilometry was reported in [6]. The intensity change with time was a sinusoidal waveform on each point of the object surface, and the height distribution on the object was proportional to the frequency of the intensity change.

Since the Fourier transform was used to obtain the frequency of the intensity change, the wavenumber or the reciprocal of the fringe period must be increased exactly at the same interval. Also in multiperiod fringe projection, a similar method using the intensity change and its frequency was reported in [9]. A method using the phase change on each measurement point was reported in [7], which is called the temporal phase-unwrapping method. Interference fringes with different periods were projected on the object surface at different times. The wrapped phase values measured during the scanning of the fringe period were unwrapped along the time axis on each measurement point. The height of the object surface on each point was obtained from the total value [8] of the phase change, which occurred during the scanning of the fringe period. The measurement accuracy of this method using the total value is not so high because only the two phase values at the largest and the smallest fringe periods are used and the intermediate phase values are discarded. In [9] these intermediate phase values were used to estimate the gradient of the phase change, which provided the height of the object surface in the same way as that in multiwavelength interferometers. Several methods using multiperiod fringe projection were compared through numerical simulations and very simple experiments in [9,10]. It is important for achieving a higher measurement accuracy to use effectively all phase values obtained during the scanning of the fringe period. Another important thing in the temporal phase-unwrapping method is how to realize a constant phase point where the phase of the fringe pattern does not change while the period of the fringe pattern is scanned. For example, in [8] the rotation axis of the mirror was used as the constant phase point. The exactness of the constant phase point directly affects the measurement accuracy.

In this paper a multiperiod fringe projection is executed with an interferometer in a similar way to [8]. However using sinusoidal phase-modulating interferometry enables us to produce exactly the constant phase point of the fringe pattern by a phase-lock technique [14]. The constant phase point produced electrically in this paper has higher accuracy than that produced mechanically in [8]. Amplitudes and phases of the fringe patterns with different periods on the object surface are detected by using sinusoidal phase-modulating interferometry [15]. Optical fields of the different fringe periods on the object surface are made from the detected amplitudes and phases. Since the optical fields on the constant phase point are not changed during the scanning of the fringe period, the optical fields on each point of the object surface are backpropagated to the constant phase point. When the backpropagated fields reach the constant phase point, the amplitude of the sum of the backpropagated fields with the different fringe periods becomes maximum and its phase becomes zero. The backpropagation distance from each point of the object to the constant phase point provides the position of the object surface. This method is hereafter

called the backpropagation method. Simulations make it clear that measurement results by the backpropagation method are not sensitive to noises contained in the measured phase. Although the backpropagation method needs a long computation time, it achieves a measurement accuracy higher than the other methods in the multiperiod fringe projection. In experiments, a step profile made by gauge blocks and a step profile made by aluminum plates are measured. It is confirmed in the experiments that a distance of several millimeters can be measured with a high accuracy of several micrometers by using the backpropagation method in the multiperiod fringe projection.

2. Principle

A schematic for the multiperiod fringe projection interferometry is shown in Fig. 1. Two plane waves of wavelength λ propagating in different directions produce a parallel interference fringe in the space. The coordinate system (x_p, y_p, z_p) is involved with the fringe pattern as shown in Fig. 1. The intersecting angles between the two waves and the z_p axis are $\pm\theta_m$, respectively. The period of the fringe pattern is expressed by $P_m = \lambda/2\theta_m$ since $\sin \theta_m \approx \theta_m$ when θ_m is small. Changing the intersecting angles θ_m as $\theta_0, \theta_1, \dots$, and θ_{M-1} , the periods of the fringe pattern P_m are scanned as P_0, P_1, \dots , and P_{M-1} accordingly. The phase of the interference fringe at $x_p = 0$ is kept at $\pi/2$ during the period scanning by using a feedback control system. The phase distribution in the coordinate system (x_p, y_p, z_p) is written as

$$\alpha_m(z_p, x_p) = k_m x_p + \frac{\pi}{2}, \quad (1)$$

where $k_m = 2\pi/P_m$, and it is called the wavenumber of the fringe pattern.

It is assumed that there is a point object Q on the surface of the object. An image of the point is formed

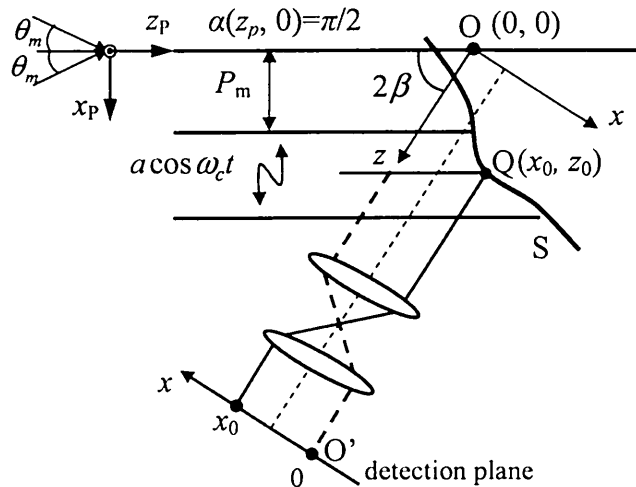


Fig. 1. Schematic for multiperiod fringe projection and detection of the fringe patterns by sinusoidal phase-modulating interferometry.

on a detection plane with an afocal imaging system. Another coordinate system (x, y, z) involved with the imaging system is defined. The original O of the coordinate system (x, y, z) is the same as that of the coordinate system (x_p, y_p, z_p) . The z axis is parallel to the optical axis of the imaging system. The intersection angle of the axis z_p and the axis z is 2β . The phase distribution in the coordinate system (x, y, z) is written as

$$\alpha_m(x, z) = k_m(x \cos 2\beta + z \sin 2\beta) + \frac{\pi}{2}. \quad (2)$$

The position of the point object Q is expressed by $x = x_0$ and $z = z_0$. The magnification of the imaging system is assumed to be a unit for the sake of simplicity. The size of an object is limited to less than the aperture of the afocal imaging system. The position of $x = 0$ on the detection plane corresponds to the original O and the image of the point object Q is formed at $x = x_0$ on the detection plane. The interference fringe intensity oscillates sinusoidally in the direction of the x_p axis with the form of $a \cos \omega_c t$ in order to incorporate the sinusoidal phase-modulating interferometry. Then the following interference signal produced by the point object Q is detected on the detection plane:

$$I_m(x_0, t) = A_m + B_m \cos[a \cos \omega_c t + \alpha_m(x_0, z_0)], \quad (3)$$

$$m = 0, \dots, M - 1.$$

The amplitude B_m and the phase α_m of the interference signal are calculated with the sinusoidal phase modulation method. The calculated value of $\alpha_m(z_0)$ is wrapped in the range between $-\pi$ and π . Since the original point of the coordinate x on the detection plane is decided by finding a position where the phase α_m is a constant value of $\pi/2$ during the scanning of the fringe period, the coordinate x_0 of the object is provided by the position of the detection plane. The following phase α_{mz} is extracted from the phase $\alpha_m(x_0, z_0)$ by subtracting the value of $k_m x_0 \cos 2\beta + \pi/2$ from the calculated value of $\alpha_m(z_0)$:

$$\alpha_{mz}(z_0) = k_m z_0 \sin 2\beta. \quad (4)$$

The range of $\alpha_{mz}(z_0)$ is between $2n\pi - \pi$ and $2n\pi + \pi$, where n is an integer value and the component of $2n\pi$ is removed from the $\alpha_{mz}(z_0)$. Since the coordinate x_0 of the object is known, a method that is called the backpropagation method is used to get the coordinate z_0 of the point object.

In the backpropagation method, the detected field of the point object Q is made as

$$D_m(x_0, z_0) = B_m \exp[j\alpha_{mz}(z_0)]. \quad (5)$$

When the detected field D_m is backpropagated to a position z , the backpropagated field of $U_m(x_0, z)$ is given by

$$U_m(x_0, z) = D_m \exp[-j\alpha_{mz}(z)], \quad m = 0, \dots, M - 1. \quad (6)$$

The sum of the backpropagated fields over all of k_m produces the following reconstruction field as a function of the backpropagation position z :

$$U_R(z) = \sum_{m=0}^{M-1} U_m(z) = \sum_{m=0}^{M-1} A_m \exp[-jSk_m(z - z_0)], \quad (7)$$

where S is the incline coefficient that is written as $S = \sin 2\beta$ and k_m is the wavenumber of the fringe pattern. k_m is expressed as $k_m = k_0 + m\Delta k$, where Δk is the scanning interval of k_m . If A_m and z_D are denoted by $A_m = 1$ and $z_D = z - z_0$, Eq. (7) is reduced to

$$U_R(z) = \exp\left\{j\left[-k_0 + \frac{(M-1)}{2}\Delta k\right]Sz_D\right\} \frac{\sin\left(\frac{M}{2}\Delta kz_D S\right)}{\sin\left(\frac{1}{2}\Delta kz_D S\right)} \quad (8)$$

$$= A_R \exp(j\phi_R).$$

Therefore the amplitude A_R of U_R is given by

$$A_R = \frac{\sin\left(\frac{B_k}{2} z_D S\right)}{\sin\left(\frac{\Delta k}{2} z_D S\right)}, \quad (9)$$

where $B_k = M\Delta k$ is the scanning range. When z_D is close to zero, Eq. (9) can be approximated as $A_R = M \sin(MWz_D)/(MWz_D)$, where $W = \Delta k S/2$. The phase distribution ϕ_R of U_R is given by

$$\phi_R = \left[-k_0 + \frac{(M-1)}{2}\Delta k\right]Sz_D = -k_C Sz_D, \quad (10)$$

where $k_C = k_0 - [(M-1)/2]\Delta k$ is the central wavenumber.

From Eqs. (9) and (10), the amplitude of A_R becomes maximum and its phase ϕ_R becomes zero at $z_D = 0$ where z is equal to the coordinate z_0 of the point object Q . From this basic characteristic, the coordinate z_0 of the object point Q can be obtained.

Now the measurement of the surface profile S of an object is considered as shown in Fig. 2. The coordinate z of each point on the surface of the object is calculated with the backpropagation method described above. To get the height distribution of the surface, a reference plane AB is defined as shown in Fig. 2. The intersecting angle between the reference plane and the coordinate x is β so that the interference fringe reflected by the reference plane propagates in the direction of the z axis, which is the optical axis of the imaging system. The coordinate x_r of the reference plane corresponding to the object point Q is expressed as

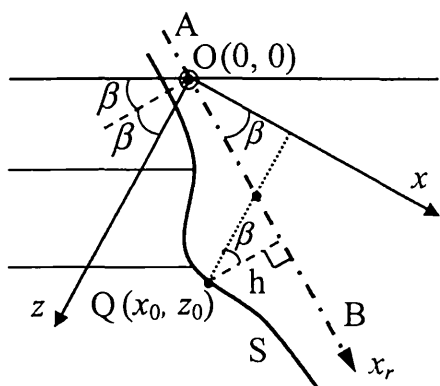


Fig. 2. Height h from standard plane AB in measurement of surface profile S .

$$x_r = x_0 \cos \beta + z_0 \sin \beta. \quad (11)$$

The height h normal to the reference plane on a point (x_r, y_r) is given by

$$h(x_r, y_r) = (z_0 - x_0 \tan \beta) \cos \beta. \quad (12)$$

3. Numerical Analysis

Characteristics of the backpropagation method are discussed in this section. The scanning interval of k_m is given by

$$\Delta k = \frac{2\pi}{M-1} \left(\frac{1}{P_0} - \frac{1}{P_{M-1}} \right) = \frac{(k_{M-1} - k_0)}{M-1}. \quad (13)$$

Since $U_m(z)$ is a discrete function with respect to k_m , $U_R(z)$ becomes a periodic function with respect to z . Considering Eqs. (4)–(7), the period of $U_R(z)$ or the measurement range of z is given by [11]:

$$z_{\max} = \frac{2\pi}{\Delta k S}. \quad (14)$$

The phase ϕ_R changes linearly with respect to z , and its period, which is called the central period, is given by Eq. (10):

$$P_C = \frac{2\pi}{k_C S} = \frac{2P_0 P_{M-1}}{(P_0 + P_{M-1})S}. \quad (15)$$

Figure 3 shows the simulation results of the backpropagation method. The scanning period of the fringe is from 200 to 400 μm with $M = 6$, $\Delta k = 0.0031$ (rad/ μm), $\beta = 45^\circ$, and $z_{\max} = 2000$ μm . The value of z_0 is 1525 μm . The amplitude B_m of the interference signal is a constant value of 1 for all P_m . Figure 3 indicates that the amplitude distribution A_R of U_R has a maximum value at $z = z_A$ and its phase distribution ϕ_R has a zero value at $z = z_\phi$ with the period P_C of 266.7 μm . When there is no error in the measurement, the values of z_A and z_ϕ are equal to the position z_0 of the point object.

It is assumed that the measured phase distribution α_m contains a measurement error that has a normal

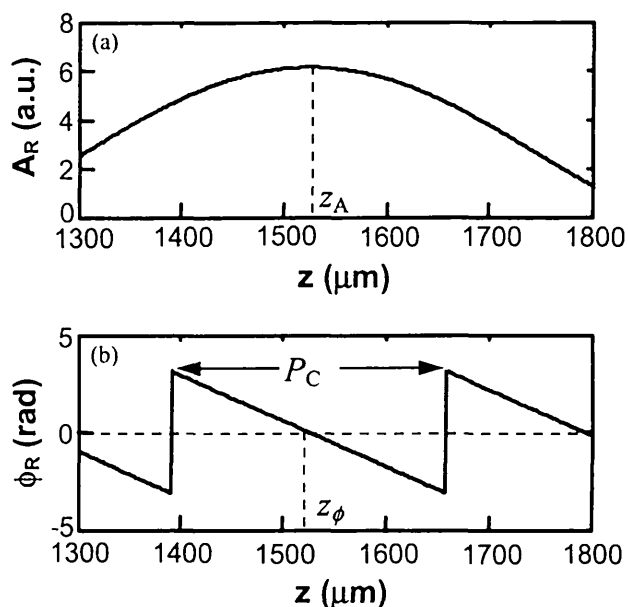


Fig. 3. Simulation results of the backpropagation method for one point object. (a) Amplitude distribution, (b) phase distribution.

distribution function with the average value of zero and the standard deviation value of σ . The simulation results in the condition of $\sigma = 0.36$ rad are shown in Fig. 4. In this case, both values of z_A and z_ϕ are different from the real value of z_0 , where $z_A = 1579$ μm and $z_\phi = 1531$ μm . Therefore the position of z_ϕ is not greatly affected by the noise compared to the position of z_A . The accurate value of z_0 is obtained from the position of z_ϕ where the difference between z_A and z_0 is less than $P_C/2$.

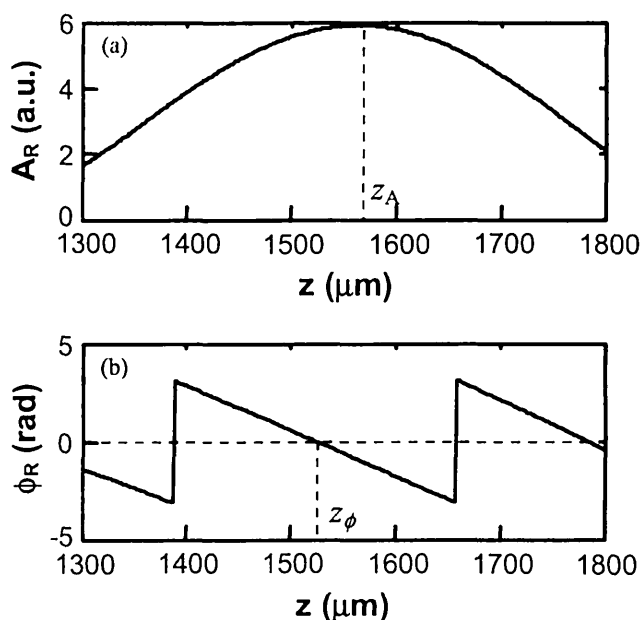


Fig. 4. Simulation results of the backpropagation method when the measured phase distribution contains a measurement error with standard deviation σ of 0.36 rad. (a) Amplitude distribution, (b) phase distribution.

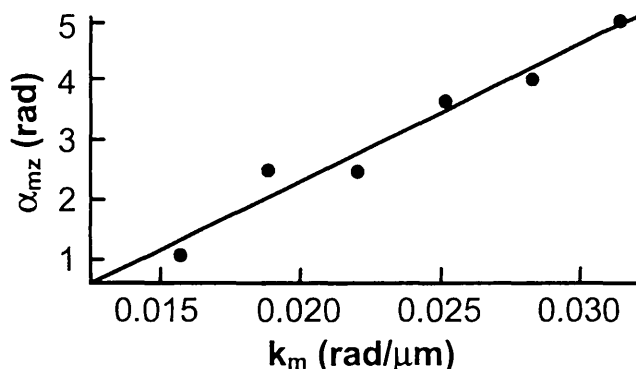


Fig. 5. Unwrapped result of measured phase distribution α_{mz} , which contains a measurement error with standard deviation σ of 0.36 rad.

The phase gradient of the measured phase distribution α_{mz} is also used to get the position z_0 of the object. In the method using the phase gradient, which is called the phase gradient method hereafter, the phase distributions α_{mz} obtained from the interference signal are unwrapped with respect to different values of k_m as shown in Fig. 5. The values of α_{mz} shown in Fig. 5 are not on a linear line because of the noise with $\sigma = 0.36$ rad. A linear line is fitted for the values of α_{mz} with the least-squares method to obtain the phase gradient q , which is given by

$$q = \frac{\partial \alpha_{mz}}{\partial k_m} = z_0 \sin 2\beta. \quad (16)$$

The value of z_0 obtained from the value of q is denoted by z_g .

Comparing the phase gradient method and the backpropagation method, some simulations were done for the noises with the different values of σ . Two hundred trials at a fixed value of σ were carried out to obtain the average and standard deviation value of z_g , z_A , and z_ϕ . The results describing the standard deviations are shown in Table 1, where $S\{w\}$ means the standard deviation of w . It was made clear from the simulation that z_g and z_A have the same characteristics. The differences between the average value of z_A and the value of z_0 are within a few tenths of a micrometer. The differences between the average value of z_ϕ and the value of z_0 are within a few micrometers. At $\sigma = 0.36$ rad, the value of $S\{z_\phi\}$ becomes large because in some trials the difference between z_A and z_0 is larger than $P_C/2$ and the value of z_ϕ is shifted by one period P_C from a value of $\sim z_0$. The

Table 1. Standard Deviations of z_g , z_A , and z_ϕ for Different Values of σ when $z_0 = 1525 \mu\text{m}$

σ (rad)	0.06	0.12	0.24	0.36
$S\{z_g\}$ (μm)	4.7	8.6	18.1	32.8
$S\{z_A\}$ (μm)	4.7	8.6	18.1	32.8
$S\{z_\phi\}$ (μm)	0.9	2.1	4.1	20.2

standard deviation value σ of the noise in the experiment described in the next section is estimated to be ~ 0.12 rad. It is concluded that the value of z_ϕ obtained from the backpropagation method has a higher accuracy than the value of z_g .

4. Experiment

A. Experiment Setup

The experimental setup is shown in Fig. 6. A 50 mW laser diode is used as the light source. A laser beam collimated with a lens L_0 is divided into two beams by beam splitter BS1. The beams reflected from mirror M1 and mirror M2 produce the interference fringe. Piezoelectric transducer 1 (PZT1) changes the angle θ of mirror 1, which changes the periods P_m of the interference fringe. The piezoelectric transducer 2 (PZT2) vibrates with frequency f_c of 125 Hz to produce the sinusoidal phase modulation in the interference fringe. The interference fringe is divided into two parts by beam splitter BS2. One part is incident on a photo diode (PD), which detects the interference signal at one point of x_f . Considering Eqs. (1) and (3), the detected interference signal is given by

$$I_m(t, x_f) = A_m + B_m \cos(a \cos \omega_c t + k_m x_f). \quad (17)$$

In the feedback control circuit, a feedback signal of $S_f = B_m \cos(k_m x_f)$ is produced by eliminating the dc component of A_m and sampling $I_m(t, x_f)$ when $\cos(\omega_c t) = 0$. A feedback control signal made from the signal S_f is applied to the PZT2 so that S_f becomes zero by moving mirror M2. Thus the feedback control system makes the phase of the point x_f fixed at $\pi/2$ while the period P_m of the interference fringe is changed. The point x_f is defined as the origin point of the x_p axis or x axis, and the expression of Eq. (1) is realized. The other part of the interference fringe is projected on the surface of the object. The image of the object's surface is formed with the afocal imaging system whose magnification is $M_{12} = f_2/f_1$, where f_1 and f_2 are the focal length of L_1 and L_2 , respectively. A high-speed CCD camera with the frame period of

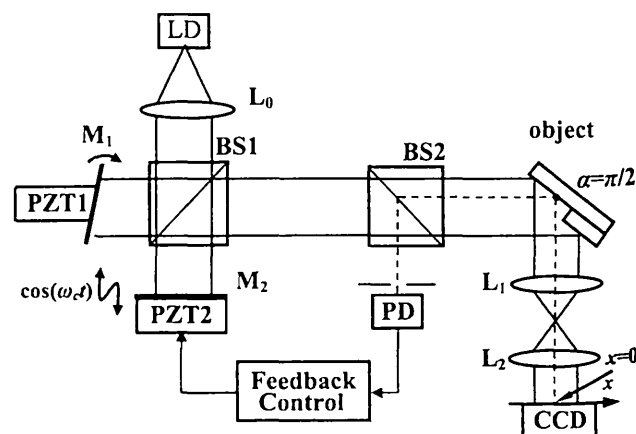


Fig. 6. Experiment setup of the multiperiod fringe projection for surface profile measurement.

1 ms is used to detect the sinusoidally phase-modulated interference fringe.

B. Experiment Results

First an optical surface with a step profile made by two gauge blocks was used as an object. Height H of the step profile was $1000\ \mu\text{m}$. The parameters used in the experiment were as follows: $P_1 = 249.8\ \mu\text{m}$, $P_2 = 285.2\ \mu\text{m}$, $P_3 = 332.6\ \mu\text{m}$, $P_4 = 400.3\ \mu\text{m}$, $\Delta k = 0.0031\ \text{rad}/\mu\text{m}$, $\beta = 45^\circ$, $z_{\text{max}} = 2000\ \mu\text{m}$, $P_C = 266.7\ \mu\text{m}$, $f_1 = 100\ \text{mm}$, and $f_2 = 50\ \text{mm}$. The image size on the x - y plane of the CCD image sensor were 256×240 pixel with pixel size of $7.4\ \mu\text{m}$, and the measuring region on the object was $\sim 3.8\ \text{mm} \times 3.6\ \text{mm}$ with $M_{12} = 1/2$. Figure 7 shows the amplitude A_R and phase ϕ_R for one measuring point of $x = 1.45\ \text{mm}$ and $y = 1.79\ \text{mm}$ on the object surface. From these results, the measured value of z_0 or z_δ was $2862\ \mu\text{m}$. The measured value of h calculated with Eq. (9) was $998\ \mu\text{m}$ at the point of $x = 1.45\ \text{mm}$ and $y = 1.79\ \text{mm}$. Figures 8 and 9 show the measured height distribution h over the reference plane and along one line of $y = 1.79\ \text{mm}$, respectively, where the notation of x_r is the x axis of the reference plane. Because of the shadow of the step profile, there is no interference signal reflected from $x_r = 0.98\ \text{mm}$ to $x_r = 1.95\ \text{mm}$. The average value of the height difference H on the line of $y = 1.79\ \text{mm}$ was $998\ \mu\text{m}$. The measurements were repeated at intervals of a few minutes. The measurement repeatability of $\sim 2.5\ \mu\text{m}$ was obtained from the rms value of the differences of the measurement results.

Next a rough surface of aluminum with a step profile was used as the object. Since the average height of the step profile was $\sim 2\ \text{mm}$, the measurement

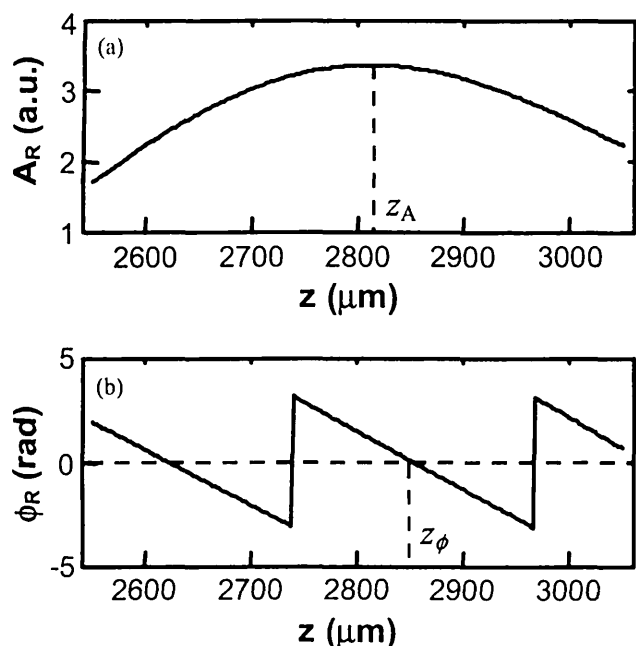


Fig. 7. Backpropagation results for one point of $x_0 = 1.45\ \text{mm}$, $y = 1.79\ \text{mm}$ on the object surface. (a) Amplitude distribution, (b) phase distribution.

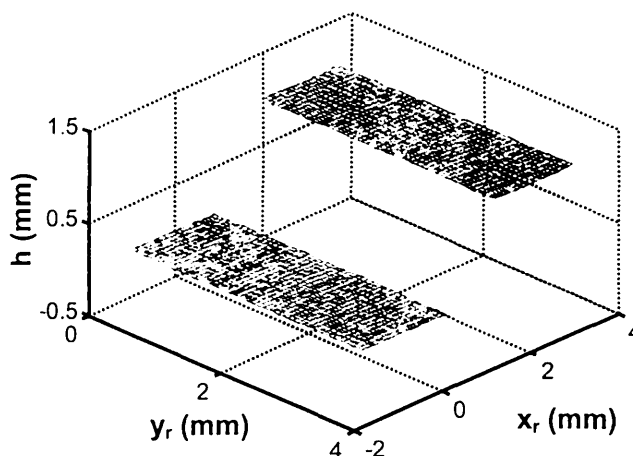


Fig. 8. Measured height distribution of the step profile made by two gauge blocks.

range z_{max} was set at $2521\ \mu\text{m}$ in the condition that the value of β was 16° and the scanning interval Δk was $0.0046\ \text{rad}/\mu\text{m}$. When β was 16° , the size of the shadow on the lower surface of the object caused by the edge point of the step profile became small. To decrease the random noise in the measurement of rough surface, the following six periods of the interference fringe were used: $P_1 = 177.9\ \mu\text{m}$, $P_2 = 205.8\ \mu\text{m}$, $P_3 = 243.3\ \mu\text{m}$, $P_4 = 297.1\ \mu\text{m}$, $P_5 = 376.2\ \mu\text{m}$, and $P_6 = 501.0\ \mu\text{m}$, where $P_C = 484.6\ \mu\text{m}$. The measuring region was $\sim 7.6\ \text{mm} \times 7.2\ \text{mm}$ with $f_1 = 100\ \text{mm}$, $f_2 = 25\ \text{mm}$, and $M_{12} = 1/4$. Figure 10 shows the height distribution of the step profile, where the height distributions of the upper and lower surfaces forming the step profile are drawn with the separated axis of h . The measured value of the height H between the central point on the two measuring surfaces of the step profile was $2070\ \mu\text{m}$. The measurement repeatability of $7.5\ \mu\text{m}$ was obtained by repeating the measurement three times at intervals of a few minutes. This repeatability was larger than that in the measurement of the optical surfaces of gauge blocks because the measure-

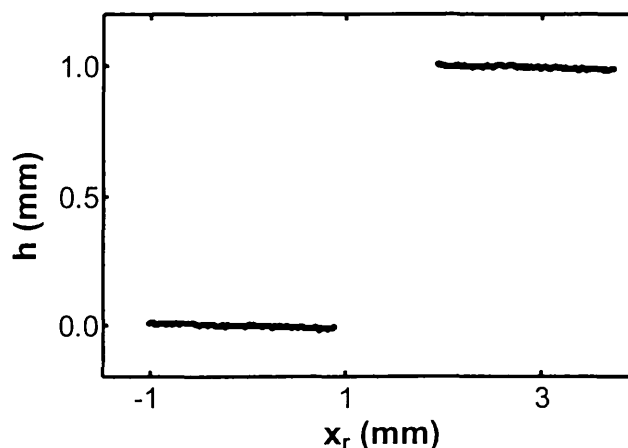


Fig. 9. Cross section of the measured height distribution of Fig. 8 at $y = 1.79\ \text{mm}$.

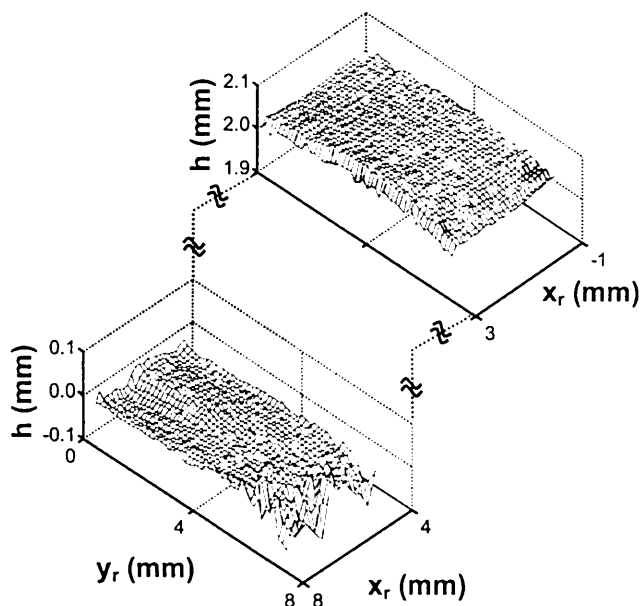


Fig. 10. Measured height distributions of two rough surfaces forming the step profile.

ment error in phase α became larger for the rough surface.

5. Conclusion

A multiperiod fringe projection interferometry by using the backpropagation method was presented. The feedback technology was incorporated to keep the phase on one point of the object surface at $\pi/2$ during the scanning of the fringe period. In the backpropagation method the optical fields with different fringe periods were backpropagated to the stationary point of the phase. The position of the object surface was obtained from the distance of the backpropagation on which the amplitude of the sum of the backpropagated optical fields became maximum and its phase became zero. The simulation made it clear that the backpropagation method had a measurement accuracy higher than the phase gradient method. The measurement repeatability was $2.5 \mu\text{m}$ for the optical surface profile with a step height of 1 mm made by the gauge blocks, and it was $7.5 \mu\text{m}$ for the rough surface profile with a step height of ~ 2 mm made by the aluminum plates.

References

1. K. Creath and J. C. Wyant, "Moire and fringe projection techniques," in *Optical Shop Testing*, D. Malacara, ed. (Wiley, 1992), pp. 653–686.
2. M. Takeda, H. Ina, and S. Kobayashi, "Fourier-transform method of fringe-pattern analysis for computer-based topography and interferometry," *J. Opt. Soc. Am.* **72**, 156–160 (1982).
3. J. E. Greivenkamp and J. H. Bruning, "Phase shifting interferometers," in *Optical Shop Testing*, D. Malacara, ed. (Wiley, 1992), pp. 501–598.
4. H. Zhao, W. Chen, and Y. Tan, "Phase-unwrapping algorithm for the measurement of three-dimensional object shapes," *Appl. Opt.* **33**, 4497–4500 (1994).
5. H. Zhang, M. J. Lalor, and D. R. Burton, "Spatiotemporal phase unwrapping for the measurement of discontinuous objects in dynamic fringe-projection phase-shifting profilometry," *Appl. Opt.* **38**, 3534–3541 (1999).
6. L. H. Jin, Y. Otani, and T. Yoshizawa, "Shadow moiré profilometry by frequency sweeping," *Opt. Eng.* **40**, 1383–1386 (2001).
7. J. M. Huntley and H. Saldner, "Temporal phase-unwrapping algorithm for automated interferogram analysis," *Appl. Opt.* **32**, 3047–3052 (1993).
8. H. O. Saldner and J. M. Huntley, "Temporal phase unwrapping application to surface profiling of discontinuous objects," *Appl. Opt.* **36**, 2770–2775 (1997).
9. J. M. Huntley and H. O. Saldner, "Error-reduction methods for shape measurement by temporal phase unwrapping," *J. Opt. Soc. Am. A* **14**, 3188–3196 (1997).
10. J. M. Huntley and H. O. Saldner, "Shape measurement by temporal phase unwrapping: comparison of unwrapping algorithms," *Meas. Sci. Technol.* **8**, 986–992 (1997).
11. S. Kuwamura and I. Yamaguchi, "Wavelength scanning profilometry for real-time surface shape measurement," *Appl. Opt.* **36**, 4473–4482 (1997).
12. C. Wagner, W. Osten, and S. Seebacher, "Direct shape measurement by digital wavefront reconstruction and multiwavelength contouring," *Opt. Eng.* **39**, 79–85 (2000).
13. H. J. Tiziani, B. Franze, and P. Haible, "Wavelength-shift speckle interferometry for absolute profilometry using a mode-hop free external cavity diode laser," *J. Mod. Opt.* **44**, 1485–1496 (1997).
14. O. Sasaki, T. Suzuki, and K. Takahashi, "Sinusoidal phase modulating laser diode interferometer with feedback control system to eliminate external disturbance," *Opt. Eng.* **29**, 1511–1515 (1990).
15. O. Sasaki and H. Okazaki, "Sinusoidal phase modulating interferometry for surface profile measurement," *Appl. Opt.* **25**, 3137–3140 (1986).